AD-A252 023

ATION PAGE

Form Approved
OMB No. 0704-0188

(2)

1. AGENCY USE ONLY (Leave blank)	2. REPORT DATE	3. REPORT TYPE AND DATES COVERED
		Final - 7/15/89-8/31/91

4. TITLE AND SUBTITLE

Superconducting Microwave Resonators for Space Applications

5. FUNDING NUMBERS

C
N00014-89-K-2034

6. AUTHOR(S)

Schone, Harlan E.

7. PERFORMING ORGANIZATION NAME(S) AND ADDRESS(ES)

Department of Physics
College of William and Mary
Williamsburg, VA 23187-8795

8. PERFORMING ORGANIZATION REPORT NUMBER

9. SPONSORING/MONITORING AGENCY NAME(S) AND ADDRESS(ES)

Naval Research Laboratory, Code 3240.HB
4555 Overlook Avenue S.W.
Washington, D.C. 20375-5000

10. SPONSORING/MONITORING AGENCY REPORT NUMBER

11. SUPPLEMENTARY NOTES

12a. DISTRIBUTION/AVAILABILITY STATEMENT

This document has been approved for public release and sale; its distribution is unlimited.

12b. DISTRIBUTION CODE

13. ABSTRACT *(Maximum 200 words)*

The research contract involved the study of high temperature superconducting microwave cavities for space applications. The focus of the program was the design, construction, testing and evaluation of an active compact hydrogen maser resonator. The critical component of the resonator is a high Q compact cavity resonator which makes use of high T_c superconductors to reduce microwave losses. By use of these materials in a compact cavity resonator, maser resonator volume can be reduced by 98% with cavity Q high enough for maser oscillation.

14. SUBJECT TERMS			15. NUMBER OF PAGES
			16. PRICE CODE
17. SECURITY CLASSIFICATION OF REPORT	18. SECURITY CLASSIFICATION OF THIS PAGE	19. SECURITY CLASSIFICATION OF ABSTRACT	20. LIMITATION OF ABSTRACT

Final Report - NRL grant #N00014-89-K-2034

The College of William and Mary held a contract for the period 15 July 1989 to 31 August 1991 under which a high Q maser resonator was constructed and evaluated for use in a space based experiment. A summary of the work is included below.

Superconducting Microwave Resonators for Space Applications

The College of William and Mary has completed a program to study high temperature superconducting microwave cavities for space applications. The focus of this program was the design, construction, testing and evaluation of an active compact hydrogen maser resonator. The critical component that enables this innovation is the development of a high Q, compact cavity resonator. The success of this high Q maser resonator is facilitated by using high transition temperature superconductors (HTS) to reduce the microwave losses in the cavity. The use of HTS in a compact cavity allows for a 98% reduction in maser resonator volume with a cavity Q large enough for maser oscillation. This will make hydrogen masers suitable for applications where size and weight are critical, such as space applications. Masers as frequency standards are needed in spacecraft for on board timing, telemetry, basic science, and navigation. The Global Positioning System (GPS) satellites would benefit from having hydrogen masers on board because, due to the excellent short term and medium term stability of active hydrogen masers, they would require less frequent time corrections than presently used clocks. This would in turn result in significantly reduced GPS-user navigation error. The details of the results can be found in the appendix, which consists of recent publications most relevant to this report.

The principal property of HTS that is useful for the hydrogen maser is its low surface resistance at microwave frequencies and at temperatures that can be reached by compact efficient refrigerators or radiant cooling. At the operating frequency of 1420 Mhz, HTS materials, namely $Y_1Ba_2Cu_3O_{7-\delta}$ (YBCO), suitable for forming large non-planar cavity structures have surface resistances about one fifth of copper at 77 K. A compact resonator made from copper has a cavity quality factor, Q_c, lower than that required to sustain oscillation [1,2,3], (The quality factor Q_c is the ratio of the stored energy to the power lost per cycle). The use of HTS in a similar cavity increases Q_c above the threshold level required for maser oscillation.

The feasibility of an HTS cavity suitable for a hydrogen maser has been demonstrated [4]. During this feasibility study, a superconducting loop-gap resonator was constructed and analyzed

[5]. The loop-gap resonator is a lumped element resonant structure inside of a shield-can. The lumped element circuit is formed by two half-cylinders, electrically isolated in the center of the shield-can [1]. The completed cavity has a volume 2% of a traditional warm maser cavity, but a Q_c significantly above the threshold needed for self oscillation. Furthermore, this cavity has been space qualified and accepted as a test device in NRL's High Temperature Superconducting Space Experiment.

The loop-gap resonator with copper electrodes measured at 77 K was found to have a quality factor of 11500. For this geometry and an operating temperature of 77 K, the maser threshold quality factor is about 14000. Using superconducting electrodes, we have demonstrated a Q_c greater than 31000. This is clearly high enough to sustain self oscillation [3]. Such a conclusion is further supported by the results of H. Wang at Hughes Research Laboratory with their oscillating compact hydrogen maser using Q-enhancement. The Q-enhancement is a feed-back loop that creates an effective cavity Q that can be several times larger than the non-enhanced Q. Hughes achieved oscillation with an enhanced Q_c that was between 20,000 and 30,000. The maser investigated during this program has approximately the same bulb size as the Hughes maser which makes the comparison meaningful. However, since Q-enhancement will increase feedback and amplify instabilities in the oscillator, the superconducting maser will be significantly more stable.

The superconducting loop-gap resonator electrodes are fabricated from silver that is electrophoretically covered with an YBCO thick film [6]. This deposition technique has also been used to create a superconducting shield-can that would further increase the Q_c and could also serve as a magnetic shield (and dc magnetic field source). Pure silver was found to be the least reactive with the YBCO, however other substrate metals with better structural properties have also been tested. Also characterized were superconducting microwave and shield-can components made with thick film YBCO on polycrystalline zirconia substrates. However, after comparing the various thick film techniques, electrophoresis on silver was most reproducible high quality thick films.

The geometry of the resonator was optimized using numerical modelling techniques. This analysis yielded the cavity design that would minimize the level of thermal fluctuations in the cavity that result in maser frequency fluctuations. The details of the numerical analysis can be found in the appendix of this report.

During this program, the results from the superconducting compact hydrogen maser resonator experiments have been the topic of three publications (one in progress) and one doctoral dissertation. The first paper on this topic, titled "A Superconducting Hydrogen Maser Resonator Made From

Electrophoretic $Y_1Ba_2Cu_3O_{7-\delta}$" won the 1990 Alan Berman Annual Research Publication Award given by the Naval Research Laboratory. The successful conclusion of the investigation has lead to three new proposals to further develop the compact maser and other closely related HTS applications.

References

1. D. B. Opie, H. E. Schone, M. Hein, G. Mueller, H. Piel, D. Wehler, V. Folen and S. Wolf, "A Superconducting Compact Hydrogen Maser Resonator Made From $Y_1Ba_2Cu_3O_{7-\delta}$", IEEE Trans. Mag., Vol. 27, 1990.

2. H. Peters, "Small, Very Small, and Extremely Small Hydrogen Maser," Proceedings of the 32nd Annual Symposium on Frequency Control, p. 469 (1978).

3. R.R. Hayes and Harry T.M. Wang, "Design for a Subcompact Q-enhanced Active Maser," Proceedings of the 39th Annual Symp. on Frequency Control, 80 (1985).

4. D.B. Opie, "A Superconducting Compact Hydrogen Maser Resonator," Doctoral Dissertation, College of William and Mary (1991).

5. D. B. Opie, et. al., A High T_c Superconducting Resonator for a Compact Hydrogen Maser," Proceedings of the 45th Annual Symposium on Frequency Control (1991).

6. M. Hein, et. al., "Electromagnetic Properties of Electrophoretic $Y_1Ba_2Cu_3O_{7-\delta}$," J. of Supercond. 3, p. 323 (1990).

A SUPERCONDUCTING HYDROGEN MASER RESONATOR MADE FROM ELECTROPHORETIC $YBA_2CU_3O_{7-\delta}$

D. Opie, H. Schone
Departement of Physics, College of William and Mary,
Williamsburg, Virginia 23185

M. Hein, G. Müller, H. Piel, D. Wehler
Fachbereich Physik der Bergischen Universität
D 5600 Wuppertal 1, West Germany

V. Folen, S. Wolf
Naval Research Laboratory, Washington DC 20375

Abstract

A compact loop-gap hydrogen maser resonator has been constructed by electrophoretic deposition of $YBa_2Cu_3O_{7-\delta}$ (YBCO) onto silver. The resonator is tuned to operate at the hyperfine transition frequency of hydrogen (1.42 GHz). This device is considered to be the first step towards a superconducting cavity for a compact hydrogen maser to be used in the Global Positioning System (GPS). The required miniaturization of the resonator reduces its Q value. This effect can be compensated for by the low surface resistance of YBCO at 77 K. Large and curved polycrystalline YBCO layers can be obtained by the electrophoretic deposition technique. In this contribution we report on the construction and the test of three loop-gap resonators which are prepared for the High Temperature Superconductor Space Experiment (HTSSE). The loop-gap electrodes are the lossiest parts of such a resonator . In a first step these electrodes with a surface of 150 cm^2 were covered with YBCO. The Q values of the resonators at 77 K ranged between 2.3 10^4 and 3.1 10^4 and exceed the minimum requirement for a later maser application. They correspond to a surface resistance between 0.7 and 1.4 mΩ which is a factor of 3 to 5 below the equivalent value of copper. The cavities can be excited in a higher order mode (HOM) at 4.3 GHz whose field distribution is still sensitive to the superconducting electrodes. Thus the experimental requirements for the HTSSE project can be fulfilled.

Introduction

The miniaturization of passive microwave components is one of the first applications of high temperature superconductors. In this report we describe the construction and first tests of a superconducting compact hydrogen maser resonator. This resonator is fabricated by covering suitably shaped silver electrodes with a layer of YBCO using an electrophoretic process [1]. The theory and techniques of the hydrogen maser are described by Kleppner et. al. [2,3]. One of the most important applications of a hydrogen maser is its use as a stable clock. One interesting example for the use of highly stable clocks concerns a global positioning system which is presently based on cesium beam atomic clocks. An exchange of these devices against hydrogen masers could improve the precision of the system significantly. The development of a compact superconducting cavity hydrogen maser was therefore proposed by two of the authors (V. Folen and S. Wolf). They proposed to replace the very large TE_{011} cavity (diameter = height = 27.6 cm) by a compact loop-gap resonator similar to that originally suggested by H. E. Peters [4] for a conventional compact maser and to fabricate this cavity from high T_c superconducting material. On the basis of their proposal a collaboration between the Physics Departement of the College of William and Mary, the Naval Research Laboratory and the Physics Department of the University of Wuppertal is developing such a cavity. It is presently foreseen as one of the devices to be tested in space within the HTSSE project.

In the first section of this report we outline the basic principle of the hydrogen maser and the concept of the loop-gap resonator. Then the electrophoretic coating of the resonator with YBCO is described. In the last section we discuss the results of experiments with three prototype cavities for the HTSSE project.

The miniaturized maser resonator

A hydrogen maser which is used as a frequency standard stimulates the emission of photons between the ground state hyperfine levels (F=1, m_f=0) and (F=0, m_f=0) of atomic hydrogen, corresponding to a frequency of approximately 1.42 GHz. Figure 1 shows the schematic of a compact hydrogen maser using a loop-gap resonator [4]. Molecular hydrogen is dissociated in a radiofrequency (rf) field and forms an atomic beam which passes through a state selecting magnetic field. Only atoms in the states (F=1, m_f=0) and (F=0, m_f=0) are focussed and enter a storage bulb where they stay for a fraction of a econd before escaping. During that time they are frequently reflected from the teflon coated quartz walls of the bulb. In a classical hydrogen maser the storage bulb is placed in a cylindrical copper cavity excited in the TE_{011} mode and tuned to the transition frequency. Stimulated emission occurs if the beam intensity is sufficient and the cavity is coherently excited in the TE_{011} mode. This only happens if the microwave losses in the cavity are low enough, which implies that its Q value is above a certain threshold. The detailed balance between beam intensity, storage time, effective volume of the storage bulb and the microwave properties of the cavity is discussed in the literature [3]. The cavity is surrounded by a magnetic shield. A proper operation of the maser requires a very small but uniform

Manuscript received September 24, 1990.

IEEE Trans. Mag. v. 27, 1990

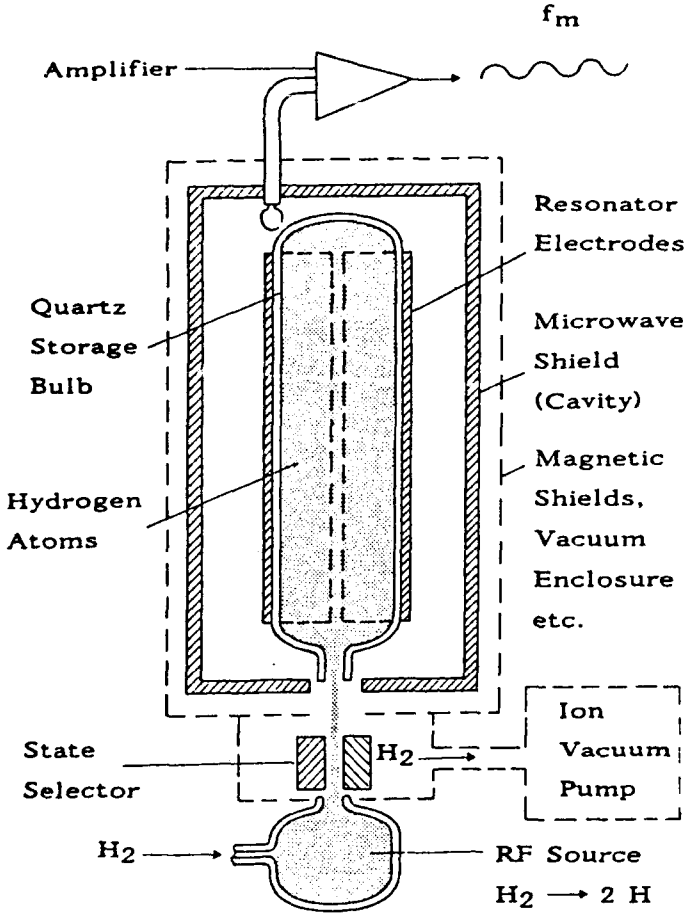

Figure 1. Schematic of a compact hydrogen maser using a loop-gap resonator [4].

d.c. magnetic field to be superimposed to the stimulating microwave field. All the other, mainly electronic components which make a hydrogen maser to be a frequency standard shall not be discussed here.

For the GPS sattelite application of the hydrogen maser the size of a traditional TE_{011} mode cavity is considered to be too large. For space applications therefore this cavity shall be replaced by a loop-gap resonator [4] similar to the one shown in figure 1. In this miniaturized design the resonator Q is significantly reduced, and maser oscillation is possible only by introducing means of Q enhancement. The discovery of the high T_c superconductors made such an enhancement possible. Fabricating the loop-gap resonator from YBCO should improve its Q compared to a copper cavity of the same geometry. The principle of the room temperature loop-gap resonator is described elesewhere [4]. Figure 2 shows our version of a superconducting loop-gap resonator for hydrogen maser application. It consists of two parts: the loop-gap electrodes with an inner diameter of the equivalent cylinder of 5 cm and an equal length, and the outer rf shield with an inner diameter and an inner length of 7.2 cm. The width of both gaps is 0.4 cm. The real and displacement currents in the loop-gap electrodes flow like in a solenoid and produce a uniform magnetic field on the inside of the half cylinders. The electrode structure is supported by two interlocking teflon cylinders and is held fixed in a concentric position inside the rf shield. The surface of these electrodes causes 76 % of the power dissipation in the maser resonator. The remaining 24 % of the losses occur on the surface of the rf shield and in the dielectric. To avoid dielectric losses, the teflon support material has been removed from the regions near the gap where the electric field is concentrated. In a first step to develop a fully superconducting loop-gap resonator the electrodes were designed to be superconducting. The two half cylinders were fabricated from silver and were then electrophoretically covered on both surfaces with a polycrystalline YBCO layer of about 20 µm in thickness. The applied technique is described in the next section. The rf shield was fabricated from OFHC copper. For the HTSSE project this shield acts as a hermetically sealed can with two microwave couplers and at the same time as a connection to the cold finger of the refrigeration system.

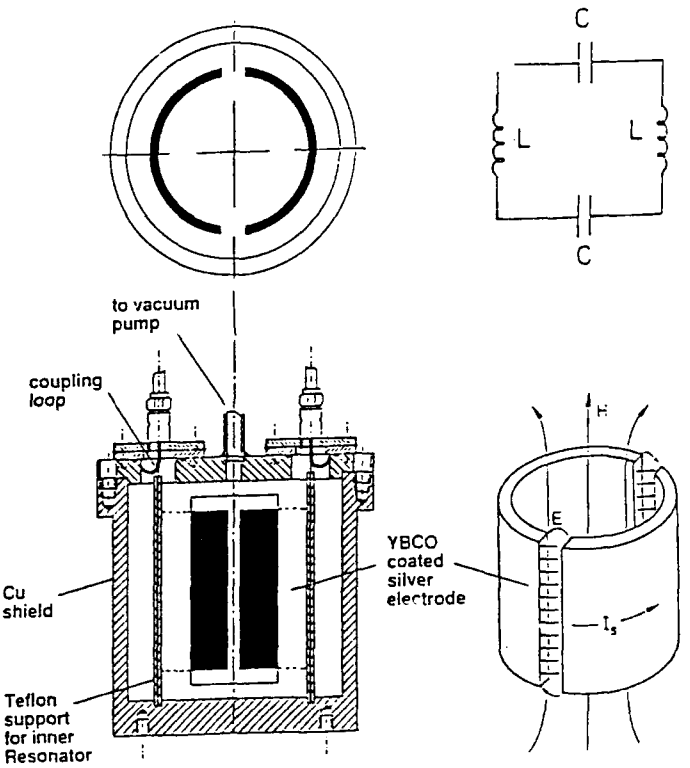

Figure 2. Schematic of a compact loop-gap maser resonator with the field configuration at the inner electrodes and the equivalent circuit.

For a successful maser application the geometry of the storage bulb, the Q value of the cavity, the distribution and concentration of the microwave field within the hydrogen volume (referred to as filling factor) and the operating temperature are decisive parameters [2-4,6]. Considerations of the balanced choice of these parameters have only guided our work. The main objective of this experiment is the demonstration of a significant improvement in Q by taking superconducting YBCO instead of copper, especially at 1.4 GHz in the described loop-gap arrangement.

In order to be space tested this resonator should also fulfill the requirements of the HTSSE project. Therefore, due to the limited frequency range covered by the HTSSE electronics, a resonant mode had to be found between 4 and 5 GHz. Such a field configuration is given by that TEM mode where the resonator is seen as a coaxial line of length λ with the electrodes acting as the inner and the rf shield as the outer conductor. The length of both conductors was chosen to obtain a resonant frequency of 4.3 GHz for this higher order mode. The influence of the dielectric within the rf shield causes a frequency drop of 0.5 GHz compared to the analytically expected resonant frequency of 4.8 GHz. This field configuration is excited mainly in the space between the electrodes and the rf can and senses only the outer surfaces of the loop-gap electrodes. Nevertheless, its sensitivity will be sufficient to observe a possible degradation of the cavity performance during the space test.

The electrophoretic coating with YBCO

We have applied the electrophoretic effect to cover the two loop-gap electrodes with a textured YBCO layer. The technique of the electrophoretic coating procedure of silver substrates with YBCO and the obtained results for the surface resistance of such layers are described in detail elsewhere [1,5]. Here we give only a schematic description of the process.

After preparing a fine YBCO powder with the correct 1:2:3 metal stoichiometry we produced a suspension by adding 10 to 20 g of the powder to 100 ml pure aceton. Two cylindrically bound and concentrically arranged silver sheats acted as anodes. The half cylinders which were covered separately, were mounted between the anodes with a mutual distance of about 1.5 cm. Applying an appropriate voltage [5], both inner and outer surfaces were covered simultaneously with a thin YBCO layer of about 5 µm in thickness. To produce a preferential orientation of the migrating YBCO particles, a d.c. magnetic field of 8 T parallel to the axis of the half cylinders was applied during the deposition.The colloidal powder particles which are essentially single crystals are oriented with their c-axis parallel to the magnetic field and are deposited in this texture. Each depositon step was followed by a drying step and a subsequent sintering period of about 1 h at 900 to 920 ^{o}C in oxygen. The deposition and sintering steps were repeated 4 times until a resulting layer thickness of about 20 µm was accumulated. This iterative procedure is adopted to cover cracks in the YBCO layer which develop during sintering. Finally, the YBCO layers were sintered for 140 h at a temperature programmed to vary between 920 and 930 ^{o}C in oxygen and then slowly cooled to room temperature. As confirmed by electron microscopy, the resulting layers show a significant texture with the c-axis parallel to the cylinder axis. Thus, the currents for the solenoidal field of the maser mode, depicted in figure 2, flow preferentially within the ab-planes of the crystallites forming the polycrystalline YBCO surface of the loop-gap electrodes. As found in earlier experiments [5], this texture favours a reduced surface resistance.

Cryogenic tests, results and discussion

For the HTSSE project three loop-gap resonators were fabricated so far. Each resonator was tested by mounting it to an appropriate cryogenic test system within a helium bath cryostat. The interior of the cavity was evacuated and then filled with low pressure helium gas (10^{-3} mbar at 4.2 K) to provide a thermal contact between the inner electrodes and the copper shield. The cavity was cooled to 4.2 K by filling the cryostat with liquid helium. Then the helium was removed and the cavity warmed up to room temperature within 48 h. The cavity temperature was monitored by a platinum resistor. Its Q was determined by a computer controlled sweep of the drive frequency and by measuring the full width at half maximum of the transmitted power. The main results of the three experiments are summarized in table 1.

Table 1. Summary of the microwave properties of three loop-gap resonators investigated in the maser mode (1.4 GHz) and a higher order mode (HOM, 4.3 GHz).

	cavity A	cavity B	cavity C
maser mode			
Q (300 K)	630	660	650
Q (77 K)	28000 ± 2000	31000 ± 3000	23000 ± 2000
Q (4.2 K)	(1 ± 0.1) 10^5	not measured	not measured
HOM			
Q (300 K)	1200	1100	1100
Q (77 K)	23000 ± 2000	31000 ± 3000	34000 ± 3000
Q (4.2 K)	57000 ± 5000	not measured	not measured

For economic reasons cavities B and C were tested only at temperatures above 77 K. The temperature dependence Q (T) of the same cavity fabricated from OFHC copper was also measured. From these measurements the temperature dependence of the surface resistance, $R_S(T)$, of YBCO as well as of Cu was determined at the maser frequency. For the higher order mode, the geometry constants needed for the determination of R_S can presently only be estimated. At 1.4 GHz, the Q value of the Cu cavity was 5000 at room temperature and 12000 at 77 K. From table 1 it is seen that the superconducting loop-gap resonator (superconducting electrodes within a Cu shield) has a Q at 77 K which is about 6 times higher than the Q of the Cu resonator at 300 K, Q (Cu, 300 K), and still more than two times higher than Q (Cu, 77 K). Figure 3 shows $R_S(T)$ at 1.4 GHz for cavity A. In figure 4 we compare the results for R_S of the three loop-gap resonator experiments to the best results obtained so far on polycrystalline YBCO samples. It should be kept in mind that each pair of electrodes exposes a surface of 150 cm^2 to the microwave field. A detailed review on the microwave properties of high T_c superconductors and the appropriate references are given in another report to this conference [7].

At 77 K and 1.4 GHz, R_s is found to be (0.9 ± 0.1) mΩ for cavity A which is a factor of four lower than the 3.8 mΩ obtained for electropolished Cu at the same temperature and frequency. The Q (77 K) for a loop-gap resonator which is completely covered by YBCO is therefore expected to be a factor four higher than an equivalent Cu device. Compared to a room temperature Cu resonator, this improvement factor even increases up to an order of magnitude. Although the operation of a hydrogen maser at 77 K asks for a higher Q than required at room temperature, a significant miniaturization benefit can be expected by using a superconducting YBCO loop-gap resonator.

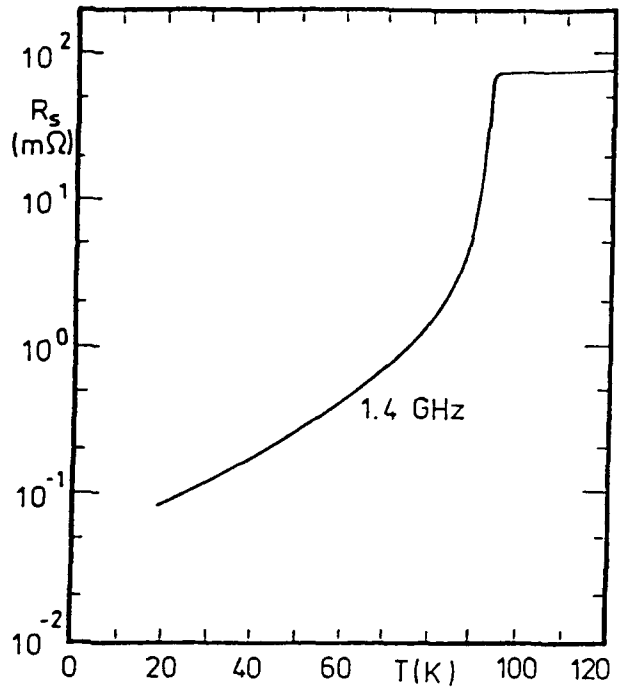

Figure 3. Temperature dependence of the surface resistance of the inner electrodes of the maser cavity for the 1.4 GHz maser mode.

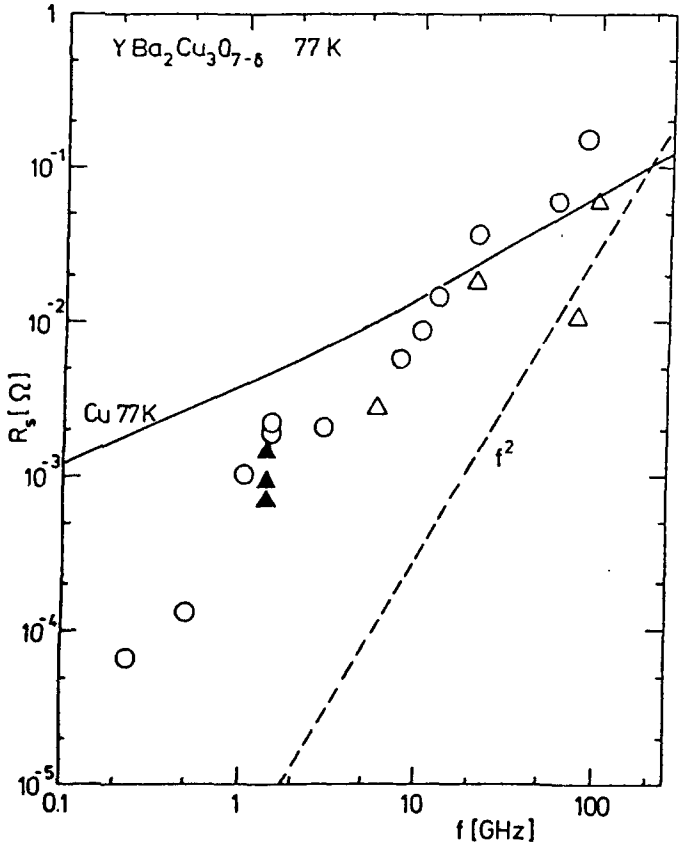

Figure 4. Surface resistance data from the maser cavity experiments (filled triangles) compared to results obtained by other groups [7] with polycrystalline untextured (circles) and textured (open triangles) YBCO as a function of frequency at 77 K.

Acknowledgements

We would like to thank H.- P. Schneider for his valuable support during the testing of the resonators. The work performed at the College of William and Mary has been funded in part by the Naval Research Laboratory. The work done at the University of Wuppertal has been funded in part by the German Minister of Research and Technology (BMFT) under the contract number 13 N 5502.

References

1. M. Hein, G. Müller, H. Piel, L. Ponto, U. Klein, M. Peiniger, "Electrophoretic deposition of textured $YBa_2Cu_3O_{7-\delta}$ films on silver substrates", *J. Appl. Phys.* 66, 5940, 1989

2. D. Kleppner, H. M. Goldenberg and N. F. Ramsey, *Phys. Rev.* 126, 603, 1962

3. D. Kleppner, H. C. Berg, S. B. Crampton and N. F. Ramsey, *Phys. Rev.* 138, A 972, 1965

4. H. E. Peters, "Small, very small and extremely small hydrogen masers", *Proc. of the 32nd Annual Symp. on Frequency Control*, 469, 1978

5. M. Hein, S. Kraut, E. Mahner, G. Müller, D. Opie, H. Piel, L. Ponto, D. Wehler, M. Becks, U. Klein and M. Peiniger , "Electromagnetic properties of electrophoretic $YBa_2Cu_3O_{7-\delta}$ films", *J. Supercond.* Vol. 2, No. 3, 323, 1990

6. M. Desaintfuscien, J. Viennet and C. Andoin, "Discussion of temperature dependence of wall and spin exchange effects in the hydrogen maser", *Metrologica* 13, 125, 1977

7. H. Piel and G. Müller, "The microwave surface impedance of high temperature superconductors", *contributions to this conference*

FORTY-FIFTH ANNUAL SYMPOSIUM ON FREQUENCY CONTROL

A High T_c Superconducting Resonator for a Compact Hydrogen Maser

D. B. Opie, H. E. Schone
College of William and Mary, Williamsburg, VA 23185

M. Hein, G. Müller, H. Piel, H.-P. Schneider
University of Wuppertal, Wuppertal, Germany

V. Folen, A. Frank, W. M. Golding, S. Wolf
Naval Research Laboratory, Washington D.C., 20375

Abstract

The advent of high T_c superconductors (HTSC) has made feasible the application of superconductivity to practical microwave devices. The measured surface resistance, R_s, of the new HTSC materials is lower than that of copper measured at the same temperature, $77K$, and frequency, 1.42GHz. An interesting application of these new materials is the miniaturization of microwave cavity resonators. In this report we describe the development, testing and evaluation of a superconducting compact hydrogen maser resonator made from electrophoretic $Y_1Ba_2Cu_3O_{7-\delta}$ (YBCO). This compact loop-gap resonator, based on a previously suggested maser resonator [1], is made superconducting using an electrophoretic process developed for the deposition of thick film polycrystalline HTSC on large non-planar metallic substrates. At $77K$ we obtain cavity quality factors comparable to those of standard size, room temperature TE_{011} maser resonators. The fields of the resonator have been studied using numerical techniques to determine the dependence of the filling factor, η', and the cavity quality factor, Q_e, on the geometric parameters. This information is used to optimize the cavity design with respect to the effects of thermal radiation on the maser performance at $77K$.

Introduction

The development of hydrogen masers as atomic clocks for space applications requires that the size and weight of the maser physics package be held to a minimum. For these applications the standard maser resonator, a cylindrical cavity operated in the TE_{011} mode at 1.42GHz, is prohibitively large. A miniaturized resonator made of non-superconducting material, but otherwise similar to the one described in this paper, is used in a compact hydrogen maser developed under NRL contract by Hughes [2]. In that maser the technique of Q enhancement or active feedback is necessary to attain sustained oscillations in the room temperature physics package. The superconducting resonator described here was designed to achieve sustained maser oscillations at $77K$ in a small package without the need for active feedback. The use of YBCO coated electrodes has made it possible to obtain the high Q_e values necessary for self oscillation within the miniaturized maser cavity.

Briefly, the operation of the maser is as follows: A beam of spin polarized atomic hydrogen is allowed to enter the interaction region of a microwave resonator which is tuned to the hyperfine transition at 1420.405MHz. The atoms are trapped in the interaction region by a Teflon coated storage bulb. The storage bulb increases the effective observation time of the atoms, thus narrowing the observed atomic linewidth. Collisions with the wall of the storage bulb and spin exchange collisions between hydrogen atoms limit the minimum achievable atomic linewidth. Provided that the atomic resonance line is narrow enough and the cavity Q is sufficient, maser oscillation is obtained. The hydrogen maser is described in detail elsewhere [3, 4].

In figure 1 we show the design of the superconducting loop-gap resonator. It consists of two parts: the loop-gap electrodes, and the outer rf shield-can. The two half cylinders are the electrodes, which behave as inductive elements. The gaps between the electrodes act as capacitive elements. This combined resonant

CH2965-2/91/0000-467 $1.00 © 1991 IEEE

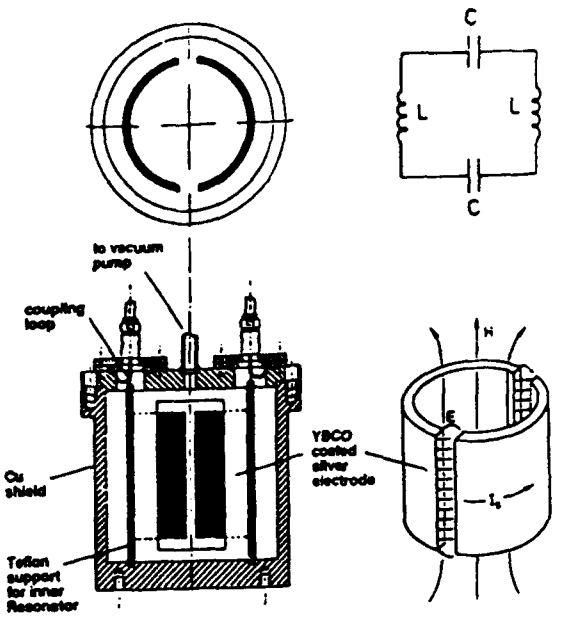

Figure 1: Schematic of a compact loop-gap maser resonator with the field configuration near the inner electrodes and the equivalent circuit.

structure largely determines the resonant frequency of the cavity. The electrodes are supported by two interlocking teflon cylinders and are held fixed, in a concentric position inside the rf shield-can. The rf currents flow azimuthally, as in a solenoid, and produce a nearly uniform axial rf magnetic field within the atomic interaction region, which is the cylindrical volume between the electrodes. The electrode surface currents account for 75% of the power losses in the maser resonator. The remaining losses occur on the surface of the rf shield-can and in the teflon support material. To reduce the dielectric losses, the teflon material has been removed from the high electric field regions near the $4mm$ wide electrode gaps.

The rf shield-can is constructed from OFHC copper and also serves as the vacuum container. Both the inner diameter and the length of the electrodes are $5.0cm$. The rf shield-can diameter and length are both $7.5cm$ producing a cavity volume of $331cm^3$. The loop-gap resonator has only 1.5% of the volume of the standard maser resonator.

The stability of an atomic frequency standard is measured by the square root of the Allan variance of fractional frequency fluctuations, $\sigma_y(\tau)$, where τ is the sampling time of the measurement [5]. The frequency fluctuations may be divided into two classes: systematic and random [6]. Systematic fluctuations are dependent on the quality of the isolation between the oscillator and the environment. Temperature changes, mechanical vibrations, and changes in the dc magnetic field are disturbances which cause systematic fluctuations. Random fluctuations are due to fundamental noise processes such as the thermal radiation within the microwave cavity and the thermal noise added by amplifiers.

It is difficult to predict the stability limitations due to systematic effects. However, the portion of $\sigma_y(\tau)$ that is limited by the cavity thermal noise within the atomic linewidth, which we call $\sigma_l(\tau)$, is predictable. The cavity design is optimized for minimum $\sigma_l(\tau)$.

Electrophoresis

Electrophoresis is the migration of charged particles under the influence of an applied electric field. It is used to coat the electrode structure of the loop-gap resonator with YBCO. The electrophoretic process allows for greater flexibility in the size and shape of the substrate than thin film deposition techniques. In this process grains of YBCO powder are colloidally suspended in a polar medium (for example, acetone or butanol) producing a positive surface charge on each grain. Under the influence of an applied electric field, these grains will move towards the negatively charged cathode, depositing themselves on its surface. This deposition process has been described in detail elsewhere [7].

The first step toward developing a fully superconducting loop-gap resonator is covering silver electrode half cylinders electrophoretically with a $20\mu m$ polycrystalline layer of YBCO. The deposition structure consisting of the silver substrate and the anode are immersed in the YBCO solution. A voltage is applied between the electrodes (figure 2) for 30 to 60 seconds to achieve a 5 to 10 μm thick layer. It is preferable to have the c axis of the YBCO crystal oriented perpendicular to the direction of the current flow because of the anisotropic current carrying properties of the YBCO. To achieve this orientation, the deposition is done in a 7 Tesla applied magnetic field. Due to the magnetic anisotropy in the room temperature YBCO

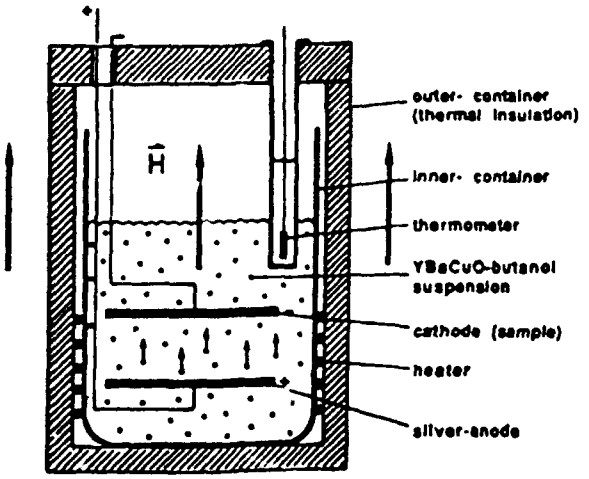

Figure 2: Diagram of an electrophoretic deposition set-up for the fabrication of textured thick films of the YBCO material.

grains, the YBCO is deposited with the c axis parallel to the direction of the applied magnetic field. The substrate and film are post annealed at $930°C$ in flowing oxygen for approximately 120 hours. This magnetic texturing technique yields lower R_s values than randomly oriented YBCO thick film samples.

Several pairs of superconducting electrodes have been made by this procedure. These electrodes have nearly $200cm^2$ of non-planar surface area. The surface resistance dependence on temperature is plotted in figure 3. At 1.42GHz and $77K$, the surface resistance is about $1m\Omega$, while the residual resistance measured at $4K$ is less than $100\mu\Omega$. The measured Q_e of the superconducting resonator at $77K$ is 30,000 which is sufficient for maser oscillation in a compact maser without the need for Q-enhancement. An identical resonator built using copper electrodes and operated at $77K$ would have a Q_e of 12,000 and require external feedback to provide Q-enhancement for oscillation.

The Loop-gap Resonator

The loop-gap resonator is a variation of the magnetron resonator which originated as early as 1935 [8]. The applications and characteristics of the loop-gap design have been discussed in more than 15 articles over the past decade. Applications for this design are found in nuclear magnetic resonance, electron spin resonance, radar, and maser spectroscopy at frequencies from 200MHzto 11GHz. The compact hydrogen maser resonator using the lumped element loop-gap design was originally suggested by H. E. Peters [1].

Empirical relations for the frequency and quality factor can be obtained as a function of resonator geometry. No analytic solution for this resonant mode exists. Recently, a technique [9] was developed to approximate the fields inside and outside the electrodes. It yields considerable agreement between measured and calculated values of the fields away from the electrodes. However this technique ignores the greatly enhanced field density at the edges of the electrodes. Without accounting for these enhanced fields incorrect values of R_s are obtained for the YBCO electrodes. Moreover, the filling factor of the maser resonator cannot be calculated properly without first understanding this effect.

It should be noted that, although the current distribution on the surface of the electrodes is solenoidal, the classical picture of a solenoid is an inadequate approximation. Since a solenoid has flux lines that can close *through* its body, the high frequency boundary conditions in the loop-gap will force all flux lines to close around the ends of the conductor and not through the electrode surfaces – resulting in a substantially different distribution of currents.

The loop-gap resonator is analogous to the shielded stripline which is a coaxial transmission line of rectangular cross section. It is also similar to the microstrip transmission line. The relations between these three models are depicted in figure 4. The currents and the fields for the three similar structures can be described as TEM. The geometry of the loop- gap can be obtained from the shielded stripline geometry by rotating the cross section of the stripline about the horizontal axis and letting the radius of the ground plane go to zero. The axis of rotation becomes the $z-axis$ of the loop-gap resonator and the center conductor of the stripline becomes the electrode structure of resonator.

The boundary conditions for the loop-gap resonator are the same as those of the shielded stripline. The rf magnetic field distribution of the loop-gap cavity is equivalent to the resonant magnetic field of the shielded stripline. The magnetic field encircles the electrodes as the equivalent field encircles the center conductor of the stripline. The electrode gaps may be neglected due to the displacement currents in the region of the gap. For the range of frequencies considered the fields are TEM and propagating in the azimuthal direction between the electrodes and the rf shield.

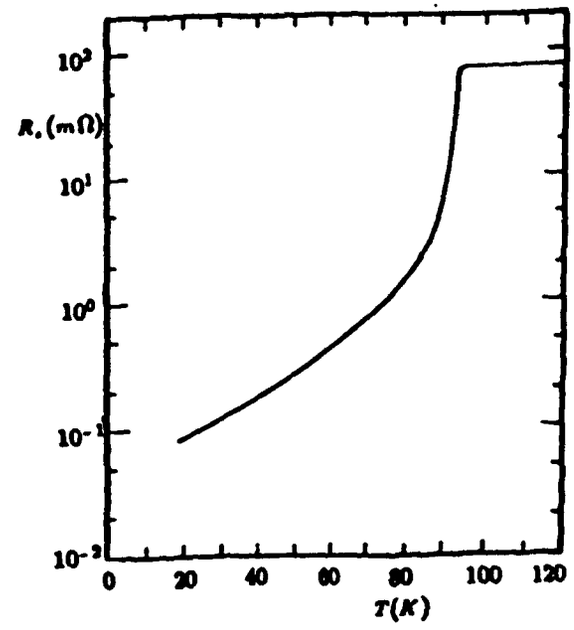

Figure 3: The temperature dependence of the surface resistance of the inner electrodes in the maser cavity measured at 1.42GHz.

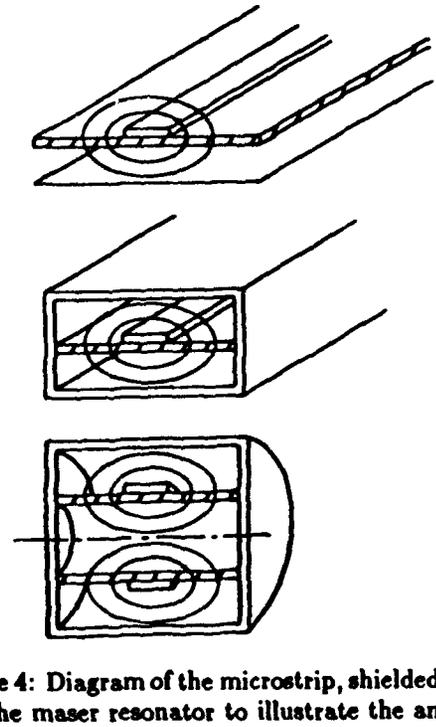

Figure 4: Diagram of the microstrip, shielded stripline, and the maser resonator to illustrate the analogy between the three structures. TEM magnetic field flux lines are shown to be similar for each case

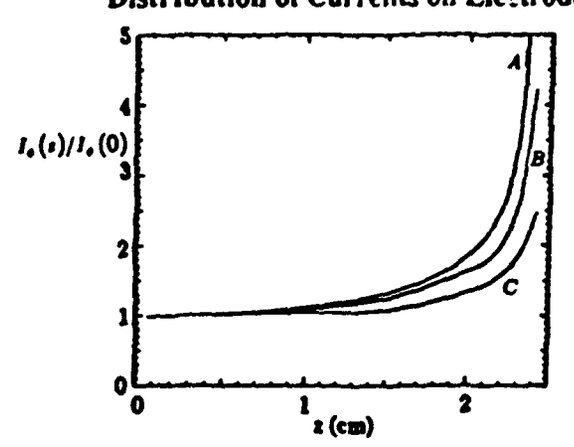

Figure 5: Distribution of the currents calculated along the $\hat{z}$ axis using three different methods: (A) conformal mapping, (B) Green's function, (C) finite element calculation.

Many attempts have been made to solve for the fields around a strip conductor. The difficulty in finding a solution to this family of problems is due to the singularities at the sharp metal corners of the finite inner conductor. However, the assumption that the conductor is infinitely thin has led to solutions that give qualitative descriptions of the fields and currents in limited cases.

As mentioned above, all of the geometries in this class of problems provide current distributions that are not constant along the strip (loop-gap electrodes) width. Specifically, the current density increases sharply at the conductor edges [10, 11, 12, 13]. This is true so long as the fields are considered to be in the "quasi-static" limit; the fields are TEM and the dimensions of the strip conductor are small compared to the wavelength. In this quasi-static limit, the current distribution is related to the distribution of excess static charge placed on the isolated strip conductor.

The relation for the currents on the microstrip is

$$I_\phi(z) = v\sigma(z) \qquad (1)$$

where v is the phase velocity and $\sigma(z)$ is the static charge distribution. The solution for an infinitely thin isolated conducting strip above a ground plane was derived by Maxwell [13]. He found that by using a conformal mapping technique, the static charge distribution on an infinitely thin conducting sheet above a

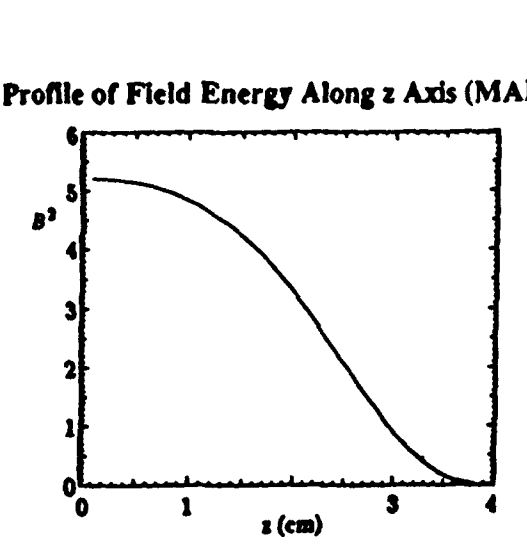

Figure 6: Profile of the magnetic field energy along the $\hat{z}$ axis where $r = 0$ showing the solenoidal field profile within the interaction region of the cavity.

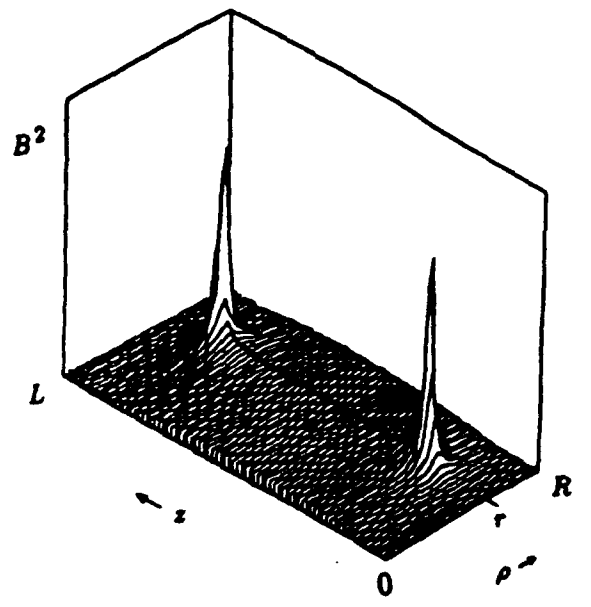

Figure 7: Plot of the field energy in the $r - z$ plane. The peaks in the energy distribution are located at the upper and lower edges of the electrodes. The relative magnitude of the fields in figure 6 are nearly too small to be seen on the scale appropriate to the peak field values.

ground plane is given by

$$\sigma(z) = \frac{\sigma_o}{\pi\sqrt{1-(2z/l)^2}}, \qquad (2)$$

where l is the width of the strip conductor and z is the point along the strip where the charge is evaluated. In this solution the current distribution is infinite but integrable at the conductor edges. A more realistic solution is found by using a Green function method [11]. The Green function and conformal mapping solutions are plotted in figure 5. Both of these solutions have the same general behavior; uniform current distribution in the center of the strip, and a sharp increase at the edges. For the shielded stripline, the edge currents on the strip are further increased by the existence of images in the shield wall [10]. This is similar to what occurs in electrostatic image problems.

A three dimensional finite difference code, called MAFIA, was used to investigate the fields in the loop-gap resonator. Plots of the magnetic and electric fields from MAFIA confirm the qualitative field descriptions reported in other loop-gap papers. As expected, the electric field is concentrated in the gap regions, and the magnetic fields are generally in the axial direction within the interaction region of the maser cavity. Figure 6 is a plot of the rf magnetic field in the center of the cavity ($r = 0$) from $z = 0$ up to the shield-can endplate, where $z = L/2$. This axial profile is very similar to the static fields of a dc solenoid and its image which is required to satisfy the boundary conditions at the endplates. However, in the regions near the electrodes, differences in the solenoid loop-gap comparison arise from the high frequency boundary conditions on the electrode surfaces. The current is distributed to satisfy these boundary conditions as shown in figure 5. Figure 7 shows the profile of magnetic field energy across the r, z plane, where $0 < r \leq R$. The enhancement of the magnetic field energy at the edges of the electrodes is as expected, and is in agreement with the stripline analogy.

The filling factor and the distribution of power losses in the resonator cannot be accurately calculated without knowing the fields. The filling factor is defined as

$$\eta' = \frac{< H_z >^2_{bulb}}{< H^2 >_{cavity}}. \qquad (3)$$

This is the ratio of the energy that stimulates the hydrogen transition to the total energy in the cavity. The approximation that the fields are uniform in the region of the electrode edges produces an optimistically large value of η'. We obtained a value of 0.39 for η' using the uniform field approximation and a value of 0.30 using the results of the finite difference code.

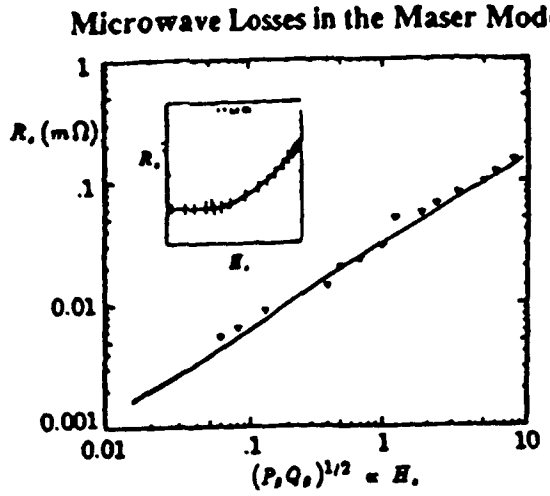

Figure 8: The surface resistance measured for the superconducting electrodes as a function of the maximum rf magnetic field on the surface of the electrodes. The expected behavior is shown in the inset indicating that at low input powers the YBCO behaves as if there is a large surface field.

The current distribution on the electrodes and on the surfaces of the shield-can vary in the same qualitative manner as in the shielded stripline. As the edges of the electrode conductor are moved closer to the shield surfaces, the currents increase due to the image currents on the shielding surfaces [11]. This change in the current distribution increases the local field energy and thereby reduces the fraction of total magnetic energy in the interaction region. The effect that this has on Q_c and η' has been studied numerically. The product $\eta' Q_c$ has a maximum where the electrode radius is about half of the shield-can radius and the electrode length is about 80% of the shield-can length.

Measuring the surface resistance in the YBCO superconducting resonator is complicated by the electrode current distribution. It has been shown that the R_s of polycrystalline YBCO is dependent on the magnitude of the rf magnetic fields at the surface [14].

The expected behavior for a cavity that does not have the unique field and current distribution shown in figure 5 is plotted as an inset in figure 8. R_s remains fairly constant with increasing surface field up to a critical value, then R_s increases sharply with further increases in the field. Figure 8 indicates that for a broad range of rf power levels, some part of the superconducting surface in the loop-gap resonator is experiencing field values beyond this critical value, even though the input power to the cavity is as low as $-30dbm$. This effect makes the characterization of the resonator surface difficult but should not cause a problem at the $-90dbm$ levels expected in an oscillating maser.

In the preceding arguments, the frequency has been assumed low enough that the wavelength is much larger than the dimensions of the strip. In this quasi-static approximation the fields are TEM and the only component of current is the azimuthal component, I_ϕ. The effect of operating at a frequency where the wavelength is on the order of the strip dimensions is that the longitudinal component of current, I_z becomes significant. It has been suggested that the form of this component is [10]

$$I_z(z) = \begin{cases} I_{z0} \sin\left(\frac{\pi z}{0.7l}\right), & |z| \leq 0.8\frac{l}{2}; \\ I_{z0} \cos\left(\frac{\pi z}{0.2l}\right), & 0.8\frac{l}{2} < |z| \leq \frac{l}{2} \end{cases} \tag{4}$$

where l is the full strip width. The magnitude of I_{z0} is proportional to the normalized strip width l/λ, where λ is the wavelength corresponding to the resonant frequency. When $l/\lambda < 0.1$, the average current amplitude I_{z0} across one half of the strip width is less than ten percent of the average $I_\phi(z = 0)$ current amplitude. For the cavity built at the University of Wuppertal, the condition that $l/\lambda < 0.1$ is not satisfied. Specifically, for an operating frequency of 1.42GHz (corresponding to a $21cm$ wavelength) and an electrode length of $5cm$, this cavity is not operating within the quasi-static limit. This would imply that in the maser resonator, the currents no longer flow only azimuthally around the electrodes but that there is a component of the current in the longitudinal (z) direction.

Shown in figure 9 is a MAFIA plot of $B_\phi(z)$ at the surface of the conductor compared with the function in equation (4). The shape of this curve is similar to that expected from a stripline where $l > 0.1\lambda$. The numerical solution confirms that the transverse magnetic fields are much smaller ($< 0.01\%$) than the longitudinal magnetic field component over most of the interaction region; therefore, this will not be a serious problem in our design. However, if the overall size of the loop-gap cavity is increased the transverse fields would become significant.

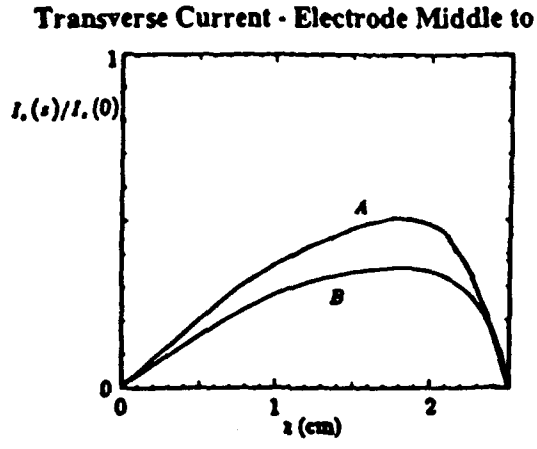

Figure 9: The component of the rf currents on the electrodes that are perpendicular to the direction of the TEM currents. The upper curve, A, is from the MAFIA calculation and the lower curve, B, is from the relationship given in reference [10].

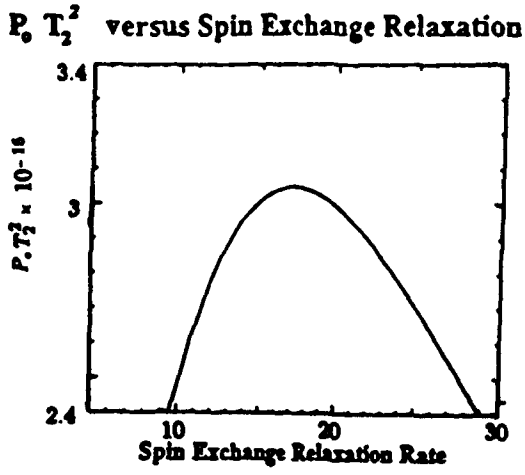

Figure 10: The product of PT_2^2 as a function of $\gamma_{1s.e.}$ which is proportional to the density of atoms in the storage bulb.

Loop-gap Design Optimization

To find the loop-gap maser resonator design that minimizes the thermal noise contributions the Allan deviation for integration times between 100 and 10000 seconds, $\sigma_l(\tau)$, must be minimized. We must express σ_l in terms of geometric variables like the resonator length L and radius R as well as the cavity quality factor, Q_c. The bulb relaxation rate, γ_b, is treated as a parameter. The spin exchange relaxation rate, $\gamma_{s.e.}$, is removed from the expressions for σ_l by minimizing σ_l with respect to $\gamma_{s.e.}$. Using these simplifications and the relationships for the filling factor and the quality factor as functions of the cavity geometry, σ_l is minimized in terms of the cavity dimensions.

The component of the Allan deviation due to the thermal noise within the cavity is given by

$$\sigma_l(\tau) \approx \frac{1}{Q_l}\sqrt{\frac{kT}{2P\tau}}. \qquad (5)$$

Where Q_l is the atomic line quality factor, k is the Boltzmann constant, T is the temperature inside the cavity, and P is the power delivered by the atomic beam to the cavity. The Allan deviation will be evaluated at $\tau = 1 second$.

Equation (5) can be rewritten as

$$\sigma_l(\tau) = \sqrt{\frac{kT}{2\pi^2 f_o^2}}\sqrt{\frac{1}{PT_2^2}} \qquad (6)$$

where $Q_l = \pi f_o T_2$, and T_2 is the transverse decay time of the atoms. The first term under the radical is not geometry dependent. Therefore it is only necessary to maximize the product PT_2^2 for the thermal noise component to be minimized. Separating out terms that are constant for changes in cavity geometry and defining these terms as the constants A and B, we have

$$PT_2^2 = BV_b\left(\frac{\gamma_1}{\gamma_2}\right)\left(A\frac{\gamma_b\gamma_{1s.e.}}{\gamma_1\gamma_2} - \frac{1}{\eta' Q}\right) \qquad (7)$$

$$A = \frac{\mu_o\mu_B^2 C_b}{\hbar\sigma v_r}$$

$$B = \frac{\hbar^2\pi f_o}{\mu_o\mu_B^2}$$

The total relaxation rates are defined as

$$\gamma_1 = \frac{1}{T_1} = \gamma_b + \gamma_{1w} + \gamma_{1s.e.} \qquad (8)$$

$$\gamma_2 = \frac{1}{T_2} = \gamma_b + \gamma_{2w} + \gamma_{2s.e.}.$$

In the above expressions, γ_1 and γ_2 are the total longitudinal and transverse relaxation rates, respectively. $\gamma_{1s.e.}$ is the spin exchange relaxation rate. As described in [4]:

$$\gamma_{1s.e} = 2\gamma_{2s.e.} \qquad (9)$$
$$= n\sigma\bar{v}_r = n\sigma 4\left(\frac{kT}{\pi m}\right)^{1/2}.$$

Here, σ is the spin exchange cross section, $\bar{v}_r$ is the average relative atomic velocity, and n is hydrogen density given by

$$n = \frac{I_{tot}T_b}{V_b}. \qquad (10)$$

γ_{1w} and γ_{2w} are the longitudinal and transverse relaxation rates due to wall collisions. p_{1w} is defined as the transverse relaxation probability per collision and τ_c is the average time between atomic wall collisions[15]. With A_b defined as the surface area of the storage container, we have

$$\gamma_{1w} = \frac{p_{1w}}{\tau_c} \approx \frac{4}{3}\gamma_{2w}$$

$$p_{1w} = 7.3 \times 10^{-6}\exp\left(\frac{230}{T}\right) = 1.45 \times 10^{-4} \qquad (11)$$

$$\frac{1}{\tau_c} = \frac{\text{mean atomic velocity}}{\text{mean free path}} = \sqrt{\frac{8kT}{\pi m}}\frac{A_b}{4V_b}.$$

Since the spin exchange relaxation rate is proportional to the hydrogen density in the bulb, we can solve for the condition of optimal density. A plot of PT_2^2 as a function of $\gamma_{1s.e.}$ is shown in figure 10. By setting the derivative of PT_2^2 with respect to $\gamma_{1s.e.}$ equal to zero and solving for $\gamma_{1s.e.}$, we find the relation between PT_2^2 and the optimal value of $\gamma_{s.e.}$ or equivalently the optimal density. This condition on $\gamma_{1s.e.}$ is substituted into equation (7). This ensures that the product of PT_2^2 is always evaluated at the optimal hydrogen density within the bulb. It is found that $\gamma_{1s.e.\ opt}$ for optimal stability is given by

$$\gamma_{1s.e.\ opt} = \frac{2(\gamma_{2w}+\gamma_b)(2\gamma_{2w}-\gamma_{1w}+\gamma_b-2A\gamma_b\eta'Q_c)}{\gamma_{1w}-2\gamma_{2w}-\gamma_b-2A\gamma_b\eta'Q_c} \qquad (12)$$

We assume that the bulb escape rate γ_b can be adjusted by changing the collimator tube length. All other variables, such as the filling factor, the bulb volume, the atomic collision rate with the walls, and the quality factor, Q_c, are dependent on the particular cavity geometry. Since no analytical solution exists for the fields in the cavity there are no analytical solutions for Q_c and η'. Therefore a numerical optimization has been performed by choosing a shield-can geometry

Limiting Stability
from Thermal Fluctuations

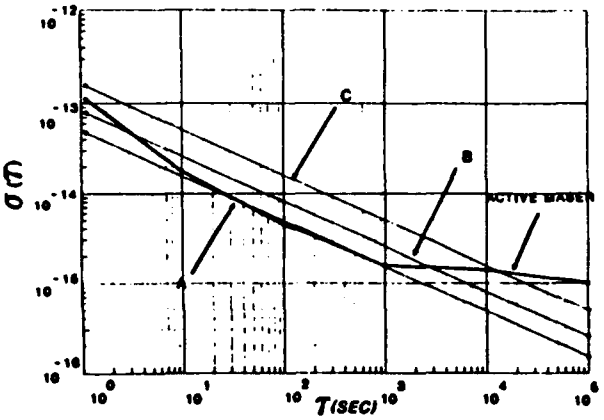

Figure 11: The Allan deviation as a function of the integration time for three different cavity geometries: (A) optimal design according to the electrode geometry for maximum PT_2^2, (B) the cavity shown in figure 1, (C) cavity designed for maximum $\eta'Q_c$. Also shown is the stability of a room temperature active maser[16]

and finding the electrode geometry that would give the best stability in that case. In order to find the optimal resonator design, many iterations of this process are needed. When PT_2^2 is considered as a function of the electrode radius and length for a given shield can geometry, there is a maximum that implies an optimal design for the electrodes. The location of this maximum is dominated by the collision rate of the atoms with the storage bulb walls. It is clear that the wall collision rate is minimized for a large bulb volume to surface area ratio.

The Allan deviation can now be calculated for any given loop-gap cavity design. The results of this calculation are shown, for three cases, in figure 11. A cavity geometry designed using the maximum $\eta'Q_c$ criteria will have a narrow storage bulb and therefore a large wall relaxation rate. This is represented by curve A in figure 11. Curve B describes the predicted level of thermal fluctuations for the cavity shown in figure 1. Curve C represents the minimum fluctuations for a cavity with a shield-can diameter and length equal to $7.5cm$ and electrodes $6.8cm$ in length and $3.2cm$ in radius. Shown for comparison is actual data from a standard active maser[16]. The level of fluctuations are reduced by a factor of three in going from the $\eta'Q_c$ geometry to the PT_2^2 maximum design where $\sigma_l(1\ second) = 6 \times 10^{-14}$.

Conclusion

A technique developed for the deposition of textured thick films of YBCO onto silver substrates of arbitrary shape has been applied to the electrodes of the loop-gap resonator. The surface resistance of the electrophoretic YBCO electrodes in this maser resonator is shown to be less than $1m\Omega$ at $77K$ and 1420MHz. Maser oscillation can now be achieved in the compact resonator without the need for Q-enhancement techniques. The design of the resonator cavity has been optimized with respect to the contribution of thermal noise to the maser oscillation using the field solutions from a 3 dimensional finite element code (MAFIA). The thermal noise within the cavity limits the stability to $\sigma_y(10000\ seconds) = 6 \times 10^{-16}$. Figure 11 shows the calculated deviations compared with fluctuations measured in a room temperature active maser. The frequency fluctuations of the optimized compact superconducting resonator coincide with these measured values. This compact superconducting maser design has frequency stability competitive with full size room temperature masers at a substantial weight and size reduction making it attractive for space applications.

Acknowledgements

We would like to thank the Research Computation Division of the Naval Research Laboratory including Kay Howell, Rob Rosenberg and Upul Obeysekare for their assistance in the finding and use of 3D Electromagnetic codes for this study. The computer department at CEBAF was also invaluable in providing computing resources for this project. This work was supported by the Naval Research Laboratory within the framework of the HTSSE project and Interatom of Germany.

References

[1] H. E. Peters, "Small, Very Small and Extremely Small Hydrogen Masers", *Proc. of the* 32^{nd} *Annual Symp. on Freq. Control*, 469, 1978.

[2] Harry T. M. Wang, "Subcompact Hydrogen Maser Atomic Clocks",*Proc. of the IEEE*, Vol. 77, No. 7, July 1989, pp. 982-992.

[3] D. Kleppner, H. M. Goldenberg and N. F. Ramsey, "Theory of the Hydrogen Maser," *Phys. Rev.*,Vol. 126, No. 2, pp. 603-615 1962.

[4] D. Kleppner, H. C. Berg, S. B. Crampton, N. F. Ramsey, R. F. C. Vessot, H. E. Peters, and J. Vanier, "Hydrogen Maser Principles and Techniques," *Phys. Rev.* A 138, 972, 1965.

[5] D. A. Howe, D. W. Allan, and J. A. Barnes, "Properties of Signal Sources and Measurement Methods", *Proc. of the* 35^{th} *Annual Symp. on Freq. Control*, pp. 1-47, 1981.

[6] E. M. Mattison and R. F. C. Vessot, "Physics of Systematic Frequency Variations in Hydrogen Masersy", *Proc.* 22^{nd} *Annual Precision Time and Time Interval Applications and Planning Meeting*, pp. 453-464, 1990 .

[7] M. Hein, S. Kraut, E. Mahner, G. Mueller, D. B. Opie, H. Piel, L. Ponto, D. Wehler, M. Becks, U. Klein, M. Peiniger, "Electromagnetic Properties of Electrophoretic $Y_1Ba_2Cu_3)_{7-\delta}$ films", J. Supercond. Vol. 3, No. 3, p. 323, 1990

[8] G. B. Collins, *Microwave Magnetrons*, York, PA., Maple Press Co., 1948.

[9] M. Mehdizadeh and T. Koryu Ishii, "Electromagnetic Field Analysis and Calculation of the Resonant Characteristics of the Loop-Gap Resonator", *IEEE Trans. Micro. Theory and Tech.*, Vol. 37, No. 7, 1989.

[10] E. J. Denlinger, "A Frequency Dependent Solution for Microstrip Transmission Lines", *IEEE Trans. Micro. Theory and Tech.*, Vol. 19, No. 1, 1971.

[11] T. G. Bryant and J. A. Weiss, "Parameters of Microstrip Transmission Lines and of Coupled Pairs of Microstrip Lines", *IEEE Trans. Micro. Theory and Tech.*", Vol. 16, No. 12, 1968.

[12] H. A. Wheeler, "Transmission-Line Properties of Parallel Strips Separated by a Dielectric Sheet", *IEEE Trans. Micro. Theory and Tech.*, Vol. MTT-13, No.2, pp. 172-185, March 1965.

[13] J. C. Maxwell, *A Treatise on Electricity and Magnetsim*, 3^{rd} ed., vol. 1, New York: Dover, 1954, pp. 296-297.

[14] G. Mueller, et al., IEEE Trans. Mag., MAG-25,p.2402, 1989.

[15] M. Desaintfuscien, J. Viennet and C. Audoin, "Discussion of the Temperature Dependence of Wall and Spin Exchange Effects in the Hydrogen Maser", *Metrologica*, vol. 13, p.125, 1977.